Research paper

Morphology, Geochemistry, and Mineralogy of Serpentine Soils under a Tropical Forest in Southeastern Taiwan

Yao-Tsung Chang,[1)] Zeng-Yei Hseu,[1,3)] Yoshiyuki Iizuka,[2)] Chun-Der Yu[1)]

【Summary】

Serpentine soils pose ecological or environmental risks because of high levels of Cr and Ni and low Ca/Mg ratios. Studies on the morphological characteristics, geochemical processes, and the mineralogical composition of serpentine soils in tropical forest ecosystems are limited. Two pedons (TK-1 and TK-2) on the ophiolite complex in the Chishang area, southeastern Taiwan, were chosen to represent the degree of soil development. The TK-1 pedon is an Entisol, whereas the TK-2 pedon is a Vertisol based on the US soil classification system. This study explored the soil morphology to establish a regional baseline for naturally occurring Cr and Ni to link to related soil geochemical properties and mineral features in this tropical forest ecosystem. The results indicated that weathering of primary minerals (i.e., serpentine and olivine) has occurred, and pedogenic Fe oxides have accumulated in the soils. However, both pedons had pH values of < 7.0, and amounts of organic carbon were low. Their cation exchange capacities were high; however, the deficiency of K in these soils may be exacerbated by the presence of clay minerals, such as mica, vermiculite, and smectite. At the exchange sites of the soils, Mg was higher than Ca, and the difference was obvious toward the bottom of the soil profile. Total contents of Cr and Ni greatly exceeded background levels in other parts of Taiwan. Clear amounts of labile Cr and Ni may have been fixed by pedogenic Fe oxides, which corresponds to the observation of serpentine mineral weathering. Concentrations of dithionite-citrate-bicarbonate-extractable Cr and Ni increased with soil development because of sorption/co-precipitation by pedogenic Fe oxides, which accumulated more in the TK-2 pedon than in the TK-1 pedon. Moreover, differences in the clay mineral composition between pedons indicate the importance of understanding the localized mineralogy when developing effective site-specific forest management strategies.

Key words: chromium, clay mineral, geochemistry, nickel, serpentine soil.

Chang YT, Hseu ZY, Iizuka Y, Yu CD. 2013. Morphology, geochemistry, and mineralogy of serpentine soils under a tropical forest in southeastern Taiwan. Taiwan J For Sci 28(4):185-201.

[1)] Department of Environmental Science and Engineering, National Pingtung Univ. of Science and Technology, 1 Shuehfu Rd., Neipu, Pingtung 91201, Taiwan. 國立屏東科技大學環境工程與科學系，91201屏東縣內埔鄉學府路1號。

[2)] Institute of Earth Sciences, Academia Sinica, 128 Academia Road, Section 2, Nankang, Taipei 11529, Taiwan. 中央研究院地球科學研究所，11529台北市南港區研究院路二段128號。

[3)] Corresponding author, e-mail:zyhseu@mail.npust.edu.tw 通訊作者。

Received August 2013, Accepted October 2013. 2013年8月送審 2013年10月通過。

研究報告

台灣東南部熱帶森林中蛇紋岩土壤之形態學、地質化學及礦物學

張耀聰[1)] 許正一[1,3)] 飯塚義之[2)] 余俊德[1)]

摘 要

蛇紋岩土壤由於鉻、鎳濃度極高且鈣/鎂比值偏低，因此具有生態與環境風險，但在熱帶森林生態系中有關蛇紋石土壤形態特徵、地球化學性質與礦物組成的研究卻不多。因此，本研究在台灣東南部池上地區選擇兩個化育程度不同的樣體(TK-1及TK-2)，在美國土壤分類系統中，樣體TK-1屬於新成土而樣體TK-2則為膨轉土。本研究目的為，探討供試土壤樣體之形態特徵，並了解此森林生態系中鉻、鎳在土壤的背景基線及其相關的地球化學過程與礦物性質。研究結果顯示，樣體中如蛇紋石及橄欖石等初生礦物被證實已開始風化，同時也伴隨次生型氧化鐵的明顯累積。然而，這兩個樣體的酸鹼值小於7.0且有機碳含量很低。雖然陽離子交換容量很高，但土壤中缺鉀的情況在雲母、蛭石及蒙特石較多時，愈是明顯。土壤顆粒表面的交換位置上鎂多於鈣，且趨近底土時鎂多於鈣的差距愈大。本研究之鉻、鎳全量遠高於台灣土壤的背景值，而隨著礦物逐漸的風化，釋出了易變動性鉻、鎳，這些鉻、鎳自礦物釋出後即與次生型氧化鐵結合。因此，連二亞硫酸鹽-檸檬酸鹽-碳酸鹽混合液所能萃取的鉻、鎳濃度在風化程度較高的樣體TK-2會高於樣體TK-1，因為透過氧化鐵吸附或共沉澱而固定了較多的鉻、鎳。再者，由於樣體間粘土礦物組成差異的重要性，突顯了森林經營管理上必須因位置不同而需要有區域特異性的策略考量。

關鍵詞：鉻、粘土礦物、地質化學、鎳、蛇紋岩土壤。

張耀聰、許正一、飯塚義之、余俊德。2013。台灣東南部熱帶森林中蛇紋岩土壤之形態學、地質化學及礦物學。台灣林業科學28(4):185-201。

INTRODUCTION

Serpentine soils are derived from ultramafic rocks and rocks with hydrothermal alteration of ultramafic minerals and a presence of serpentine minerals (Alexander et al. 2007). During metamorphic alterations of the original rock with water near the surface of the earth or in the upper part of the mantle during subduction events, anhydrous ultramafic rocks become more hydrous, and the Ca content decreases relative to the original rocks, resulting in an enrichment of Mg in serpentinites. Ultramafic rocks with abundant serpentine are defined as serpentinite (O'Hanley 1996). Serpentine is the name of a class of minerals. Serpentine-rich rocks are olive-greenish-gray and are usually blotched with stripes of various shades that resemble the skin of a snake, from which the name serpentine was derived (Brooks 1987). Serpentine rocks and soils are abundant in ophiolite belts and are typically found within regions of the circum-Pacific margin and Mediterranean Sea (Oze et al. 2004). Serpentine soils often pose ecological or environmental risks because of their high levels of potentially toxic metals, such as Cr and Ni (Hseu 2006,

Kierczak et al. 2007, Cheng et al. 2009, Bonifacio et al. 2010, Cheng et al. 2011) and low Ca/Mg ratios (McGahan et al. 2009), which interfere with various cellular functions (Wu and Hendershot 2010). Soils with high concentrations of Cr and Ni are usually toxic to plants, although they support highly specialized flora, which are rich in endemics adapted to these extreme conditions (Brooks 1998). In a number of cases, plant adaptation to soils with a high content of metals is based on mechanisms of exclusion; however, some plants actively absorb these metals at high concentrations (hyperaccumulation), often exceeding those found in the soils (Baker 1981).

Compared to other rocks, soils derived from mafic and ultramafic rocks are richer in Cr and Ni (up to 3400 mg kg^{-1} of Cr along with 3600 mg kg^{-1} of Ni); however, average concentrations of Cr and Ni in soils worldwide are approximately 84 and 34 mg kg^{-1}, respectively (McGrath 1995). Geogenic heavy metals are considered less mobile than those of anthropogenic origin in soils; however, the potential risk to the environment from serpentine soils may occur through increased bioavailability of Cr and Ni (Becquer et al. 2006, Chardot et al. 2007). Fernandez et al. (1999) indicated that sugarbeet, cabbage, and grasses in the serpentine soils of northwestern Spain accumulated considerable amounts of Cr, ranging 1.50~5.66 mg kg^{-1}, despite the fact that an average of only 0.5 mg kg^{-1} can be extracted from these soils using ethylenediaminetetraacetic acid (EDTA). Miranda et al. (2009) evaluated the accumulation of Cr and Ni in cattle that were raised in a serpentine area. Samples of the liver, kidney, and muscle of 41 animals (aged 8~12 mo) were collected at slaughter. The accumulation of Cr in the animal tissues was generally low (0.04 mg kg^{-1}) and within a normal range. However, 20% of the animal samples had toxic levels of Ni (1.30~1.77 mg kg^{-1}) in their kidneys, which is above the acceptable range (0.5 mg kg^{-1}).

The relationship between the amounts of Ca and Mg ions must be considered when assessing the required plant nutrients in a soil. The antagonism between Ca and Mg negatively affects Ca availability and plant growth (Robertson 1985). Rabenhorst and Foss (1981) found that soils with a Ca_e/Mg_e (exchangeable-form basis) ratio of < 0.1 in Maryland, USA were 98% likely to have been formed from serpentines. A recent study over large areas of a serpentine landscape in California, USA showed that serpentine soils with no detectable Ca-bearing minerals had a Ca_e/Mg_e ratio of < 0.2, whereas soils on non-serpentinitic materials had Ca_e/Mg_e ratios of > 1.0 (McGahan et al. 2009). Alexander et al. (2007) indicated that timber production of 22 serpentine soils in California was related more to the Ca/Mg ratio of the surface soil than to combinations of climatic and physical soil variables. Hence, Ca/Mg ratios have been used to infer soil genetic pathways (Lee et al. 2004) and evaluate soil fertility relationships (McGahan et al. 2009).

Serpentine minerals are abundant in the eastern part of the Central Mountain Range and Coastal Range in Taiwan, which is adjacent to the convergent boundary of the Eurasia and Philippine Sea Plates (Ho 1988). However, pedological studies of morphological characteristics, geochemical processes, and mineralogy of serpentine soils in forest ecosystems with humid tropical conditions are limited. Therefore, the objectives of this study were: (1) to explore the field morphological and micromorphological characteristics of serpentine soils with various degrees of weathering in a tropical forest of southeastern Taiwan, and (2) to establish a regional baseline for naturally occurring Cr and Ni to link

to related geochemical properties and mineral features of soils in forest ecosystems.

MATERIALS AND METHODS

Study area

The Lichi Formation on the southwestern flank of the Coastal Range is a distinct lithological unit composed of chaotic mudstones resulting from gravity sliding of marine sediments, with the additional incorporation of ophiolitic blocks during the subsequent convergence of the continental and oceanic plates in eastern Taiwan. The ophiolite complex located in the Chishang area at an elevation of 300~350 m (23°02'07''N, 121°11'29''E), Taitung County, southeastern Taiwan, was selected for this study (Fig. 1). Pyroxene groups slightly contaminated with glassy basalt are the major bedrocks in the area. Primary minerals of the regolith from the exotic blocks are mainly serpentine groups, talc, olivine, chlorite, and spinels (Chang et al. 2000). The study area is a mountain landscape with slopes of 2~10%. The climate of the area is characterized by high temperature and humidity, massive rainfall, and tropical cyclones in summer. The annual average temperature is approximately 23℃; the warmest average air temperature is approximately 30℃ in July, and the coldest temperature is approximately 16℃ in January. The seasonal variation between dry winters and wet summers creates a wet-dry tropical climate (Cwa) according to the climate classification system of Köppen (Hseu 2006). However, the annual rainfall is approximately 2000 mm and is concentrated in May to September. The soil moisture regime is udic and the soil temperature regime is hyperthermic, based on the *US Soil Survey Manual* (Soil Survey Staff 1993), and tropical broadleaf evergreen forests are the dominant vegetation, including *Acacia confusa*, *Calocedrus formosana*, and *Trema orientalis*.

Two pedons, TK-1 and TK-2, were chosen to represent the degree of soil development. Pedon TK-1 was on the convex shoulder, and pedon TK-2 was on the flat backslope. The pedons were exposed by excavating pits to the depth of the C horizon. Field

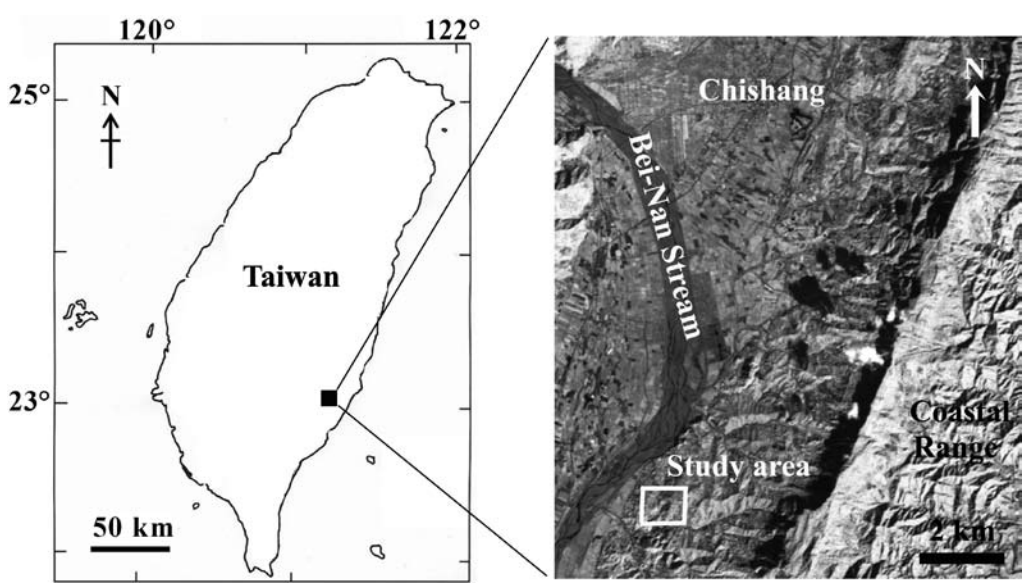

Fig. 1. Location and study area by aerial imaging.

morphological characteristics were described according to the *US Soil Survey Manual* (Soil Survey Staff 1993). Soil horizon samples were further collected, air-dried, ground, and passed through a 2-mm sieve for subsequent laboratory analyses.

Physical and chemical analyses

Bulk density was measured in undisturbed field blocks using the core method (Blake and Hartge 1986). The soil particle size distribution was determined using the pipette method (Gee and Bauder 1986). The pH of the soil was measured in a mixture of soil and deionized water (1: 1, w/v) with a glass electrode (McLean 1982). The total organic carbon (OC) content was determined using the Walkley-Black wet oxidation method (Nelson and Sommers 1982). The cation exchange capacity (CEC) was determined using the ammonium acetate method (pH 7.0), and the percentage of base saturation (BS) was calculated from CEC and the exchangeable base cations (Rhoades 1982). A dithionite-citrate-bicarbonate (DCB) extraction was applied to pedogenic Fe oxides (Mehra and Jackson 1960). The DCB extraction was also used for Cr and Ni associated with the Fe oxides (Mills et al. 2011). For the total metals analysis, 0.5 g of a sample was placed in a Teflon beaker and digested in a mixture of HF-HNO_3-$HClO_4$ modified from Baker et al. (1982). In all solutions, the metal content was determined using a flame atomic absorption spectrophotometer (FAAS) (Hitachi Z-8100, Tokyo, Japan).

Mineralogical analyses

Kubiena boxes were used to collect undisturbed soil blocks in the field. After air drying, vertically oriented thin-sections with a thickness of 30 μm were prepared by Spectrum Petrographics (Vancouver, WA, USA). Thin sections were observed for all horizons under a polarized microscope. Selected thin sections were recorded using back-scattered electron (BSE) imaging with a scanning electron microscope (SEM; JEOL JSM-6360LV, Tokyo, Japan) at the Institute of Earth Sciences, Academia Sinica (Taipei, Taiwan).

Air-dried samples were pretreated with 30% H_2O_2 to remove the organic matter and subsequently subjected to DCB treatment to remove the oxide coatings. The clay fraction was separated using the pipette method (Gee and Bauder 1986). The x-ray diffraction (XRD) analysis was performed on oriented K- and Mg-saturated clay samples. The expansion properties of the Mg-saturated samples were determined using ethylene glycol solvated at 65℃ for 24 h. K-saturated samples were further subjected to successive heat treatments of 350 and 550℃ for 2 h. The oriented clays were examined using an x-ray diffractometer (Rigaku D/max-2200/PC type, Tokyo, Japan) and Ni-filtered Cu-Kα radiation generated at 30 kV and 10 mA. The XRD patterns were recorded of 2^o to 50^o (2θ) with a scanning speed of 0.2^o (2θ) min^{-1}. Identifications of clay minerals were based on difference among reflection patterns of the K-saturated, Mg-saturated, glycolated, heated, and air-dried samples, and semiquantitative determination of minerals was achieved using differences in the diffraction intensity peak of each identified mineral under various treatments (Johns et al. 1954, Brindley 1980). Additionally, XRD patterns of the bedrock from the bottom of each pedon were obtained of $0\sim60^o$ 2θ at a rate of 0.2^o (2θ) min^{-1} using the x-ray diffractometer.

RESULTS AND DISCUSSION

Parent materials

Three polymorphs of serpentine, chrysotile, antigorite, and lizartide were found in the

serpentine soils of eastern Taiwan (Hseu et al. 2007), with similar [$Mg_3Si_2O_5$ $(OH)_4$] compositions (Caillaud et al. 2006). Microscopy using plane-polarized light showed that the dominant groundmass was serpentine in the parent materials (Fig. 2A). Moreover, antigorite and lizardite with high birefringence under cross-polarized light were demonstrated by the hourglass texture (Fig. 2B). During weathering, serpentine minerals are unstable in soil environments (Rabenhorst et al. 1982) and are characterized by fine textures (Hseu et al. 2007). This may be attributed to the fine-grained nature of the parent materials. Because of strong weathering in a tropical climate, the lizardite was altered and had generated iron stains on the mineral surface (Fig. 2C). Opaque inclusions of spinels were found in the groundmass of serpentines (Fig. 2D), which are resistant to weathering (Cheng et al. 2011).

A spinel is a mineralogical group of oxides with a general formula, AB_2O_4, where A is Fe^{2+} and B is Fe^{3+}, Al, or Cr. It is subdivided according to whether the trivalent ion is Al (spinel series), Fe^{3+} (magnetite series), or Cr (chromite series). The chromite series is known as chromian spinel or brown spinel. Pure end-members of the spinel group are rare in nature. Chromites have a wide composition range because of substitutions of Mg for Fe^{2+} and Al and Fe^{3+} for Cr (Abre et al. 2009); therefore, a wide range of Cr concentrations in chromite were reported in the related literature (15~45 Cr wt.%) (Oze et al. 2004, Kierczak et al. 2007, Hseu and Iizuka 2013). Hseu and Iizuka (2013) indicated that chromite may undergo incongruent dissolution and chemical modification to act as a crucial source of labile Cr in serpentine soils of eastern Taiwan. For the observation of thin sections in the BSE mode of SEM, spinels

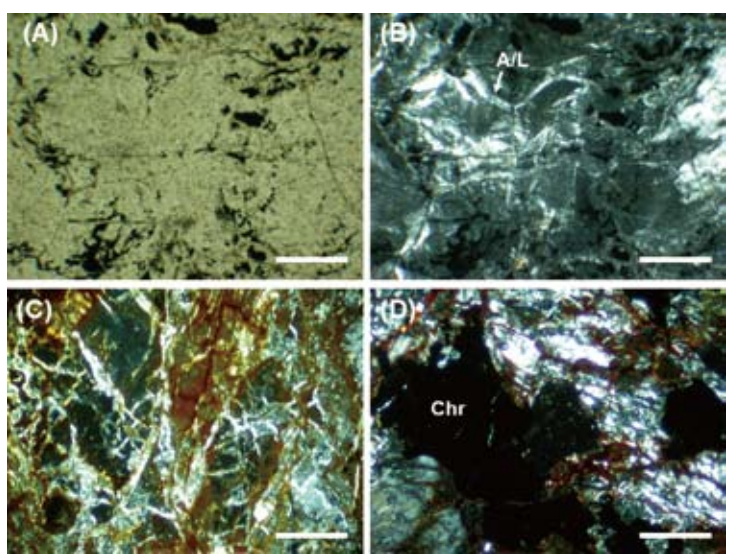

Fig. 2. Micrographs of a thin section of serpentinitic rocks. The groundmass of serpentine under plane-polarized light (A) and antigorite mixed with hourglass-textured lizardite (A/L) with high birefringence under cross-polarized light (B); weathered lizardite with iron stains under cross-polarized light (C) and opaque inclusions of chromite under cross-polarized light (D); length of the scale bar is 0.25 mm.

were easily recognizable from the surrounding serpentines because spinels appeared brighter than silicates, which indicated that the cations were heavier than silicon in the crystal lattice. Chromites exhibited cracking on the grain surfaces (Fig. 3A). In serpentine soils, the dominant source of Cr is chromian spinels, whereas the dominant source of Ni is silicates (Cheng et al. 2011, Mills et al. 2011). Ni-rich spinel is rare in serpentine soils; however, it was observed in the BSE mode of SEM (Fig. 3B). Ti/Fe-rich spinels were also observed on the surface of serpentinites (Fig. 3C). Additionally, goethite, a common pedogenic Fe oxide, had formed as needle shapes and accumulated on the surface of parent materials (Fig. 3D).

In addition to the mineral groups of serpentine and spinel in the serpentine soils, original minerals before serpentinization were found in the parent materials, such as olivine and plagioclase. The corroded serpentine exhibited morphological characteristics of initial olivine (Fig. 4A). Plagioclase, a common feldspar mineral in the crust of the Earth, is typically needle-shaped and easily weathered to produce pedogenic Fe oxides (Fig. 4B); however, plagioclase is not a series of serpentine groups. More pedogenic Fe oxides with dark-brown colors surrounding the weathered plagioclase or olivine were observed in the TK-2 pedon than the TK-1 pedon (Fig. 4C, D).

Soil morphology

The depth to the C horizon in the TK-1 pedon was only 35 cm, whereas it was 100 cm in the TK-2 pedon (Table 1). No organic surface horizon was observed in the soils; however, the surface A horizons were clay in texture with moderate granular structures. Munsell colors of the A-AC-C horizon sequence in the TK-1 pedon were dark-gray (7.5YR 3/1), dark-brown (7.5YR 3/2), and brown (7.5YR 4/4), classifying the soil as an

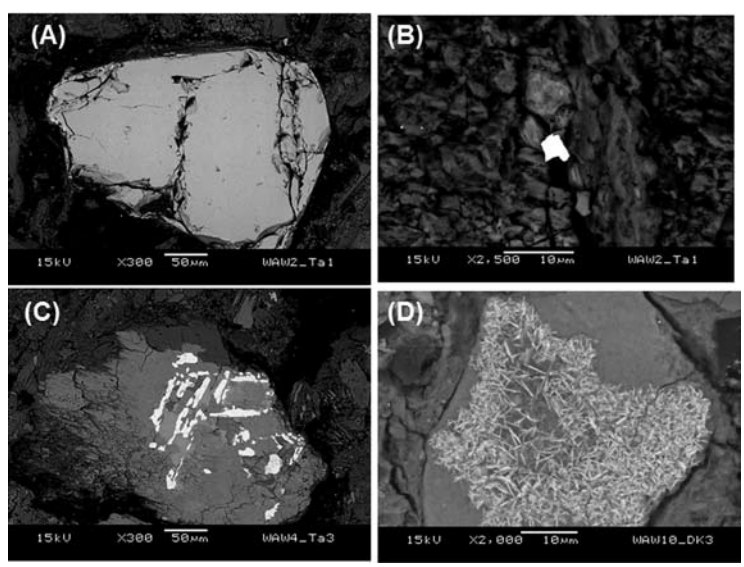

Fig. 3. SEM photographs in the BSE operating mode of a thin section. (A) Chromite in the C horizon of the TK-1 pedon; (B) Ni-rich spinel in the Bss3 horizon of the TK-2 pedon; (C) Ti/Fe spinel in the AC horizon of of the TK-1 pedon; (D) goethite in the Bss1 horizon of the TK-2 pedon.

Entisol in Soil Taxonomy (Soil Survey Staff 2010). Colors of the TK-2 pedon resembled those of the TK-1 pedon; however, some of the subsurface horizons had a higher value

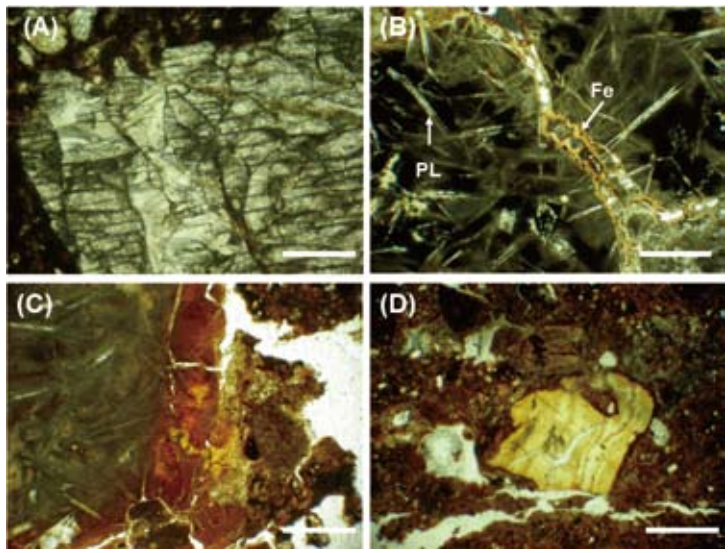

Fig. 4. Photomicrographs of a thin section from the C horizon under plane-polarized light. Serpentinized olivine with altered cracks (A) and slightly weathered plagioclase (PL) matrix in association with yellow iron (Fe) oxides along cracks (B) in the TK-1 pedon; brown Fe oxides coated on the plagioclase (C) and original olivine (D) in the TK-2 pedon; length of the scale bar is 0.25 mm.

Table 1. Morphological characteristics of the studied pedons

Horizon	Depth (cm)	Munsell color	Texture[1)]	Structure[2)]	Void[3)]	Boundary[4)]
TK-1 pedon						
A	0~20	7.5YR 3/1	C	2vf&fgr	3f&m	gs
AC	20~35	7.5YR 3/2	C	2mgr	2vf	gs
C	>35	7.5YR 4/4	C	1fsbk	1vf&f	
TK-2 pedon						
A1	0~10	7.5YR 3/2	C	2vf&fgr	2vf&f	gs
A2	10~23	7.5YR 3/2	C	2fsbk	2f&m	gs
AB	23~40	7.5YR 4/3	C	2fabk	2f&m	cs
Bss1	40~60	7.5YR 4/4	C	2f&mabk	2vf&f	ds
Bss2	60~80	7.5YR 4/6	C	2f&mabk	2vf&f	cs
Bss3	80~100	7.5YR 4/6	C	2f&mabk	1vf&f	ds
C	>100	7.5YR 5/6	C	1vf&fabk	1vf&f	

[1)] SL, sandy clay; C, clay.

[2)] 3, strong; 2, moderate; 1, weak; vf, very fine; f, fine; m, medium; c, coarse; vc, very coarse; gr, granular; sbk, subangular blocky; abk, angular block.

[3)] 3, many; 2, common; 1, few; vf, very fine; f, fine; m, medium; c, coarse.

[4)] c, clear; g, gradual; d, diffuse; s, smooth.

and chroma in the Musell color chart. In the TK-2 pedon, angular blocky structures, pressure faces, and slickensides were common and became abundant with increasing depth in all Bss horizons, indicating relatively high pedogenic development compared to the TK-1 pedon. Therefore, these field morphological characteristics met the criteria of a Vertisol in Soil Taxonomy (Soil Survey Staff 2010). The fine textures were reflected in the soil's consistency; thus, the soils were almost firm when dry and sticky and plastic when moist.

Soil physical and chemical properties

Bulk densities in all horizons ranged 0.7~1.5 Mg m^{-3} in the TK-1 pedon and 0.8~1.2 Mg m^{-3} in the TK-2 pedon, and increased with depth, partly because of roots loosening the soil, higher organic matter in the surface horizons, and overburden consolidation of the lower horizons (Table 2). The clay content was higher in the TK-2 pedon than in the TK-1 pedon, corresponding to field observations regarding the soil structure, stickiness, and plasticity.

The pH of all soils was weakly acidic (Table 2). The pH increased with soil depth in the TK-1 pedon, whereas the profile distribution of pH varied in the TK-2 pedon. The average pH of pedons was lower in the TK-2 pedon than in the TK-1 pedon. The OC content was in the range of 0.1~3.7% and decreased with soil depth; compared to a global OC database (Lee et al. 2004), the soils were low in OC. This may be attributed to rapid decomposition of the biomass under the prevalent hyperthermic temperature regime and udic conditions and inferior vegetation cover on the serpentine terrain. Soils derived from ultramafic rocks are characterized by a relatively high CEC, which ranged

Table 2. Selected physical and chemical properties of the studied pedons

Horizon	Depth (cm)	Bd[1] (Mg m^{-3})	Texture			pH	OC[2] (%)	Exchangeable bases					BS[4] (%)	Ca/Mg[5]
			Sand	Silt	Clay			CEC[3]	K	Na	Ca	Mg		
			------- (%) -------					-------- (cmol(+) kg^{-1}) --------						
TK-1 pedon														
A	0~20	0.7	20	15	65	6.1	3.7	24	0.3	0.1	5.0	5.6	46	1.1
AC	20~35	1.1	48	2	50	6.4	0.8	14	0.2	0.1	5.2	7.1	89	0.7
C	>35	1.5	50	2	48	6.6	0.1	16	0.2	0.2	4.1	8.8	84	0.9
TK-2 pedon														
A1	0~10	0.8	15	15	70	5.8	3.1	28	0.6	0.1	15	5.8	77	2.6
A2	10~23	0.9	17	14	69	5.8	1.8	28	0.6	0.8	13	10	87	1.3
AB	23~40	1.0	13	15	78	5.7	1.9	28	0.5	0.3	11	7.6	69	1.4
Bss1	40~60	1.0	16	18	66	5.7	1.0	29	0.2	0.4	11	7.7	67	1.4
Bss2	60~80	1.0	18	13	69	5.9	0.6	27	0.1	0.4	12	14	98	0.9
Bss3	80~100	1.1	20	13	67	5.9	0.2	31	0.2	0.5	12	16	93	0.8
C	>100	1.2	25	17	59	5.9	0.2	33	0.1	0.4	11	21	98	0.5

[1] Bulk density.

[2] Organic carbon.

[3] Cation exchange capacity.

[4] Base saturation.

[5] The ratio of exchangeable Ca to exchangeable Mg.

approximately 16~33 cmol(+) kg^{-1} in this study. The exchangeable bases showed relatively high amounts of Ca and Mg in all horizons, whereas Na and K were lower. The BSs were high; however, no correlation with depth was observed in the pedons.

In general, the amount of Ca obtained from soils is considerably higher than that of Mg regarding higher plant growth. However, soils derived from serpentines exhibit strong chemical fertility limitations because of the low Ca/Mg ratio. During weathering and leaching of serpentinitic soils, large quantities of Si and Mg are lost and Ca accumulates in the plant detritus (Brooks 1987). Hseu (2006) indicated that exchangeable Ca/Mg ratios in most serpentine soils in eastern Taiwan are consistently < 1.0, except for a few surface horizons. Additionally, a serpentinitic soil chronosequence in western North America exhibited a gradual decrease in the amount of exchangeable Mg with age; therefore, exchangeable Ca/Mg ratios in the profile substantially increase with the age of the soils. This increase is common in aging serpentinitic soils because plants recycle more Ca than Mg; therefore, more Mg is lost (Alexander et al. 2007). The intensity of Ca biocycling is higher in surface soils than in the subsoils in serpentinitic landscapes (McGahan et al. 2009); thus, the exchangeable Ca/Mg ratio decreased with soil depth in all pedons (Table 2). Additionally, the exchangeable Ca/Mg ratio in some subsurface horizons was < 1.0, indicating that Mg was higher than Ca at exchange sites in the soils, and the difference was more obvious toward the bottom of the soil profile. Regarding the proposed threshold value (0.7) of the exchangeable Ca/Mg ratio for nutritional balance (Brooks 1987), Ca/Mg ratios in the subsurface horizons were marginal.

Contents of Cr and Ni

Cr and Ni contents in the soils were higher than those in soils formed from other parent materials, with a considerable variation between pedons (Table 3), which may indicate the degree of chemical weathering of serpentinitic rocks (Lee et al. 2004). Levels of total Cr, which commonly occurs in ser-

Table 3. Total contents and DCB-extractable amounts of Fe, Cr, and Ni in the studied pedons

Horizon	Depth (cm)	Total			DCB		
		Fe	Cr	Ni	Fe	Cr	Ni
		(g kg^{-1})	------ (mg kg^{-1}) ------		(g kg^{-1})	------ (mg kg^{-1}) ------	
TK-1 pedon							
A	0~20	64.8	1990	1590	14.7	99.5	495
AC	20~35	72.6	2070	2690	13.0	87.6	309
C	>35	24.8	1770	3750	11.4	88.3	307
TK-2 pedon							
A1	0~10	53.8	664	878	19.3	134	812
A2	10~23	55.0	833	956	22.4	184	920
AB	23~40	59.9	811	973	17.4	136	720
Bss1	40~60	63.7	906	1030	22.0	181	745
Bss2	60~80	59.5	1010	1050	16.8	139	708
Bss3	80~100	63.6	988	1060	15.4	144	687
C	>100	70.3	605	1010	15.4	106	542

pentinites as the accessory mineral, chromite (Hseu and Iizuk 2013), vary considerably with depth. Concentrations of siderophile (iron-loving) elements, such as Cr and Ni, varied substantially in global serpentine soils (Oze et al. 2004). However, Cr concentrations were within the higher range for global serpentine soils. Ni concentrations ranged approximately 920~3748 mg kg^{-1} and directly corresponded to changes in Cr concentrations with respect to depth (r^2 = 0.61, $p < 0.05$). This result indicated that Cr accompanied Ni in serpentine soils (Hseu 2006, Cheng et al. 2011, Ho et al. 2013). However, Ni was higher than Cr in soils of subsurface horizons. Compared to prior studies, Ni concentrations were in a normal range for global serpentine soils (Cheng et al. 2009). Natural background levels of total Cr and Ni in agricultural soils of Taiwan are approximately 50 and 60 mg kg^{-1}, respectively (Jien et al. 2011). Soil control standards (SCSs) of Cr and Ni contamination are 250 and 200 mg kg^{-1}, respectively, in the *Soil and Groundwater Pollution Remediation Act* of Taiwan. Total contents of Cr and Ni greatly exceeded background levels and SCSs in Taiwan.

Proctor and Woodell (1971) suggested that researchers of serpentine soils must not rely on a total analysis to represent the extractable nutrients available to plants. Extractable element contents in soils may more accurately represent the pool of available nutrients in soils for plant growth than total elemental contents (McGrath 1995). DCB-extractable Cr ranged 87.6~184 mg kg^{-1}, whereas amounts of DCB-extractable Ni were higher than those of Cr (Table 3). DCB extraction released up to 22 and 96% of total Cr and Ni, respectively, in soils, indicating that considerable amounts of Cr and Ni were released from the parent material by weathering. Pedogenic Fe oxides are crucial sinks of Cr and Ni (Lee et al. 2004, Hseu 2006, Chardot et al. 2007, Cheng et al. 2011, Ho et al. 2013). Strong correlations were observed for Fe with Cr (r^2 = 0.88, $p < 0.05$) and Fe with Ni (r^2 = 0.82, $p <$ 0.05) with DCB extraction. These correlations demonstrated that the amounts of potentially labile Cr and Ni may have been fixed by the pedogenic Fe oxides in the serpentine soils. Moreover, amounts of DCB-extractable Cr and Ni increased with soil development because of sorption/co-precipitation by pedogenic Fe oxides, which accumulated more in the TK-2 pedon than the TK-1 pedon (Table 3).

Soil mineral composition

For the primary mineral composition, XRD analyses revealed a dominance of serpentine, which exhibited peaks at 0.72 and 0.359 nm in the bedrock of the pedon (Fig. 5). XRD peaks at 1.44, 0.72, and 0.359 nm are indicative of chlorite. In addition to serpentine and chlorite, associated silicate minerals, including amphibole, talc, and olivine, were identified by the trace peak at 0.85 nm for amphibole, 0.314 nm for talc, and 0.306 and 0.278 nm for olivine, as indicated by Hseu et al. (2007). Caillaud et al. (2006) showed that hourglass textures were derived from olivine in the serpentinite, which corresponded to the finding of olivine in Fig. 4A and 4D. Additionally, chromite was identified by XRD patterns according to the reflection peaks at 0.26 and 0.202 nm (Fig. 5).

XRD patterns of clay fractions in the AC horizon of the TK-1 pedon and Bss2 horizon of the TK-2 pedon are illustrated to explain the clay mineralogy (Fig. 6). The reflection at 25℃ in the K-saturated clays was present at 0.72 nm, and it may contain chlorite because the peak was reduced when heated to 550℃. Conversely, chlorite was clearly characterized by peaks at 1.41, 0.72, 0.478, and 0.359 nm. Chlorite was present in all horizons of both

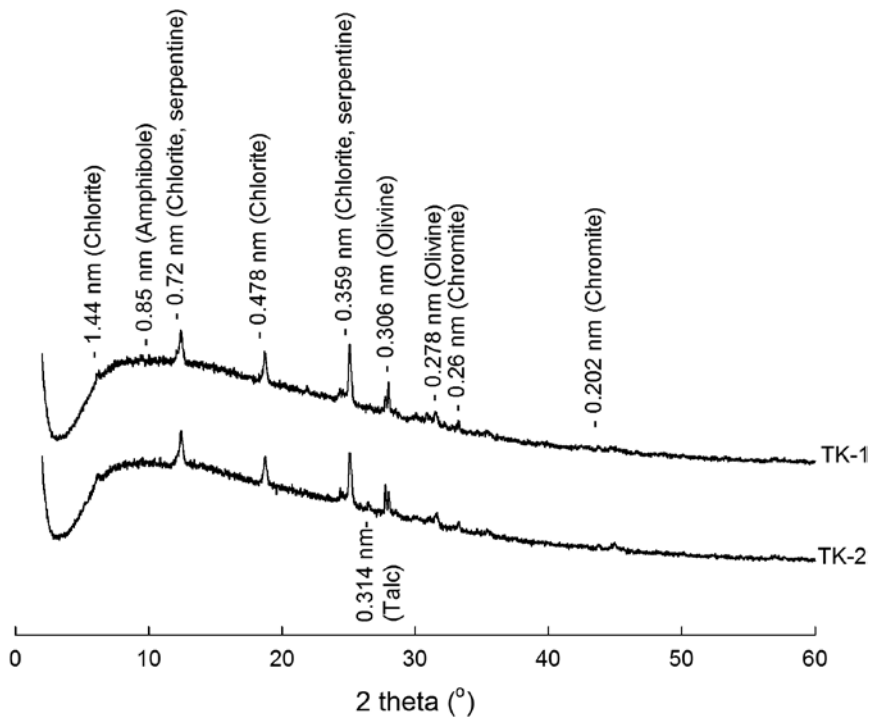

Fig. 5. XRD powder patterns of bedrock samples.

pedons; however, it increased with soil depth (Table 4). Vermiculite was characterized by a peak at 1.0 nm when K-saturated clays were heated to 350 and 550℃ and a peak at 1.41 nm when Mg-saturated clays were solvated with glycerol. Basal XRD peaks at 1.41 nm with Mg-saturated clays and intermediate between 1.2 and 1.3 nm with K-saturated clays heated to 350℃ are characteristics of randomly interstratified chlorite-vermiculite (Lee et al. 2003), which is a chlorite-like mineral; however, the interlayer OH sheet of the chlorite structure was incomplete (Hseu et al. 2007). Serpentine was also identified in the clay fraction of both pedons by a characteristic XRD peak at 0.72 nm, which persisted with K saturation and heating to 550℃. Serpentine increased with soil depth in each pedon (Table 4). Smectite was identified by its 1.4~1.5-nm spacing after Mg saturation, which increased to approximately 1.82 nm upon glycerol solvation. A chlorite and vermiculite mixture with an incomplete interlayer OH sheet was identified from its peak at 1.24 nm with K-saturation at room temperature; however, the 1.24-nm diffraction peak considerably weakened when the K-saturated sample was heated to 330 and 550℃. Mica was characterized by its peak at 1.01 nm. Chromite was also identified by XRD patterns according to reflection peaks at 0.26 and 0.202 nm (Fig. 5).

Implications for forest management

The inadequate source of K (Table 2) for sustainable plant growth may limit forest production. The deficiency of K in these soils may be exacerbated by the presence of vermiculite, smectite, and mica, which have high capacities to irreversibly retain K^+ and NH_4^+ (Banriga et al. 2011). Moreover, amounts of vermiculite, smectite, and mica were higher

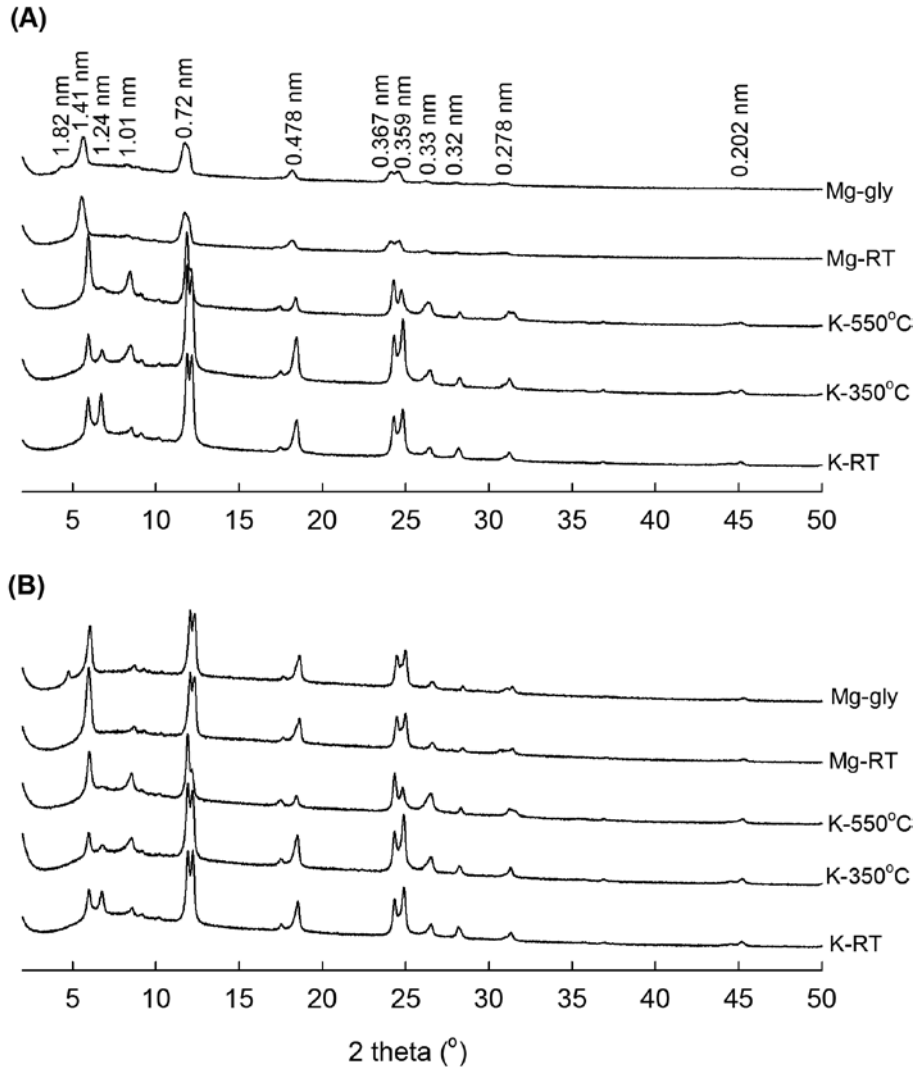

Fig. 6. XRD patterns of the clay fraction in the AC horizon of the TK-1 pedon (A) and in the Bss2 horizon of the TK-2 pedon (B) with K-saturated treatments at room temperature (RT) and 350 and 350℃ and with Mg-saturated treatments.

in the TK-2 pedon than in the TK-1 pedon (Table 4). The predominance of easily weatherable minerals, such as serpentine, chlorite, and talc, released Cr and Ni, which were sequestrated in the pedogenic Fe oxides. Additionally, chromite, a spinel strongly resistant to weathering, may undergo incongruent dissolution and chemical modification to act as a substantial source of Cr in serpentine soils of eastern Taiwan (Hseu and Iizuka 2013). The relatively high exchangeable Ca/Mg ratios present challenges to forest productivity because of nutrient imbalances and release of toxic metals into the ecosystem. According to the DCB-extractable amounts of Fe, Cr, and Ni (Table 3), high concentrations of Cr and Ni and redox-sensitive Fe oxides can affect forests and the environment when the

Table 4. Composition and semiquantitative amounts of clay minerals in the studied pedons[1)]

Horizon	Depth	CHL	SME	C-V	VER	ILL	SER
TK-1 pedon							
A	0~20	++[2)]	-	-	+	-	+
AC	20~35	++	+	+	+	+	++
C	>35	+++	-	-	-	-	+++
TK-2 pedon							
A1	0~10	+	-	+	+	+	+
A2	10~23	++	+	+	+	+	+
AB	23~40	++	+	+	+	+	++
Bss1	40~60	++	++	+	+	-	++
Bss2	60~80	++	++	+	+	-	++
Bss3	80~100	++	++	-	-	-	++
C	>100	+++	+	-	-	-	++

[1)] CHL, chlorite; SME, smectite; C-V, chlorite and vermiculite mixture; VER, vermiculite; Ill, illite; SER, serpentine.

[2)] +++, 25~50%; ++, 10~25%; +, < 10%; -, undetectable.

metals are released into the soil solution and become bioavailable. Appropriate management strategies are required to improve plant nutrition supply and balance, such as liming and application of K and Ca fertilizers. However, differences in clay mineral compositions between pedons indicate the importance of understanding the localized mineralogy to develop effective site-specific forest management strategies.

CONCLUSIONS

Both pedons had pH values of < 7.0, and the amounts of organic carbon were low under the prevalent hyperthermic temperature regime, udic conditions, and inferior vegetation cover in the area. The soils were characterized by a high cation exchange capacity; however, the deficiency of K in these soils may be exacerbated by the presence of pedogenic silicate minerals. Additionally, the exchangeable Ca/Mg ratio in some of subsurface horizons was < 1.0, indicating that Mg was higher than Ca at exchange sites in the soils, especially toward the bottom of the soil profile. Total contents of Cr and Ni in this study greatly exceeded background levels and soil control standards in Taiwan. Although Cr and Ni were geogenic in this study, clear amounts of labile Cr and Ni may have been fixed by pedogenic Fe oxides, such as goethite. However, if pedogenic Fe oxides are dissolved after the redox change in forest ecosystems, the labile Cr and Ni could be released into the soil solution and become bioavailable.

ACKNOWLEDGEMENTS

The authors would like to thank the National Science Council of Taiwan, for financially supporting this research under grant nos. NSC99-2313-B-020-010-MY3 and NSC102-2313-B-020-009-MY3.

LITERATURE CITED

Abre P, Cingolani C, Zimmermann U, Cairncross B. 2009. Detrital chromian spinels

from Upper Ordovician deposits in the Precordilleraterrane, Argentina: a mafic crust input. J S Am Earth Sci 48:407-18.

Alexander EB, Coleman RG, Keeler-Wolf T, Harrison S. 2007. Serpentine soil distributions and environmental influences. In: Alexander EB, Coleman RG, Keeler-Wolf T, Harrison S, editors. Serepntine geoecology of western North America. New York: Oxford Univ. Press. p 55-78.

Baker AJM. 1981. Accumulators and excluders – strategies in the response of plants to heavy metals. J Plant Nutr 3:643-54.

Baker DE, Amacher MC. 1982. Nickel, copper, zinc, and cadmium. In: Page AL, Miller RH, Keeney DR, editors. Methods of soil analysis, Part 2. 2nd ed. Agronomy Monographs 9. Madison, WI: Agronomy Society of America and Soil Science Society of America. p 323-36.

Bangira C, Deng Y, Loeppert RH, Hallmark CT, Stucki JW. 2011. Soil mineral composition in constrasting climatic regions of the Great dyke, Zimbabwe. Soil Sci Soc Am J 75:2367-78.

Becquer T, Quantin C, Rotté-Capet S, Ghanbaja J, Mustin C, Herbillon AJ. 2006. Sources of trace metals in Ferralsols in New Caledonia. Eur J Soil Sci 57:200-13.

Blake GR, Hartge KH. 1986. Bulk density. In: Klute A, editor. Methods of soil analysis, Part 1. 2nd ed. Agronomy Monographs 9. Madison, WI: Soil Science Society of America. p 363-75.

Bonifacio E, Falsone G, Piazza S. 2010. Linking Ni and Cr concentrations to soil mineralogy: Does it help to assess metal contamination when the natural background is high? J Soils Sediments 10:1475-86.

Brindley GW. 1980. Quantitative x-ray mineral analysis of clays. In: Brindley GB, Brown G, editors. Crystal structures of clay minerals and their x-ray identification. London: Mineralogical Society. p 411-38.

Brooks RR. 1987. Serpentine and its vegetation: a multidisciplinary approach. London: Croom Helm. 454 p.

Brooks RR. 1998. Plants that hyperaccumulate heavy metals: their role in phytoremediation, microbiology, archaeology, mineral exploration and phytomining. New York: CAB International. 380 p.

Caillaud J, Proust D, Righi D. 2006. Weathering sequences of rock-forming minerals in a serpentinite: influence of microsystems on clay mineralogy. Clay Clay Miner 54:87-100.

Chang CP, Angelier J, Huang CY. 2000. Origin and evolution of a mélange: the active plate boundary and suture zone of the Longitudinal Valley, Taiwan. Tectonophysics 325:43-62.

Chardot V, Echevarria G, Gury M, Massoura S, Morel JL. 2007. Nickel bioavailability in an ultramafic toposequence in the Vosges Mountains (France). Plant Soil 293:7-21.

Cheng CH, Jien SH, Tsai H, Chang YH, Chen YC, Hseu ZY. 2009. Geochemical element differentiation in serpentine soils from the ophiolite complexes, eastern Taiwan. Soil Sci 174:283-91.

Cheng CH, Jien SH, Iizuka Y, Tsai H, Chang YS, Hseu ZY. 2011. Pedogenic chromium and nickel partitioning in serpentine soils along a toposequence. Soil Sci Soc Am J 75:659-68.

Fernandez S, Seoane S, Merino A. 1999. Plant heavy metal concentrations and soil biological properties in agricultural serpentine soils. Commun Soil Sci Plan 30:1867-84.

Gee GW, Bauder JW. 1986. Particle-size analysis. In: Klute A, editor. Methods of soil analysis, Part 1. 2nd ed. Agronomy Monographs 9. Madison, WI: Agronomy Society of America and Soil Science Society of America. p 383-411.

Ho CP, Hseu ZY, Iizuka Y, Jien SH. 2013. Chromium speciation associated with iron and manganese oxides in serpentine mine tailings.

Environ Engin Sci 30:241-7.

Ho CS. 1988. An introduction to the geology of Taiwan: explanatory text of the geologic map of Taiwan. 2nd ed. Taipei, Taiwan: Center of Geology Survey, Ministry of Economic Affairs. 164 p.

Hseu ZY. 2006. Concentration and distribution of chromium and nickel fractions along a serpentinitic toposequence. Soil Sci 171:341-53.

Hseu ZY, Iizuka Y. 2013. Pedogeochemical characteristics of chromite in a paddy soil derived from serpentinites. Geoderma 202-3:126-33.

Hseu ZY, Tsai H, Hsi H, Chen YC. 2007. Weathering sequences of clay minerals in soils along a serpentinitic toposequence. Clay Clay Miner 55:389-401.

Jien SH, Tsai CC, Hseu ZY, Chen ZS. 2011. Baseline concentrations of toxic elements in metropolitan park soils of Taiwan. Terres Aquat Environ Toxicol 5:1-7.

Johns WD, Grim RE, Bradley WF. 1954. Quantitative estimations of clay minerals by diffraction methods. J Sediment Petrol 24:242-51.

Kierczak J, Neel C, Bril H, Puziewicz J. 2007. Effect of mineralogy and pedoclimatic variations on Ni and Cr distribution in serpentine soils under temperate climate. Geoderma 142:165-77.

Lee BD, Graham RC, Laurent TE, Amrhein C. 2004. Pedogenesis in a wetland meadow and surrounding serpentinitic landslide terrain, northern California, USA. Geoderma 118:303-20.

Lee BD, Sears SK, Graham RC, Amrhein C, Vali H. 2003. Secondary mineral genesis from chlorite and serpentine in an ultramafic soil toposequence. Soil Sci Soc Am J 67:1309-17.

McGahan DG, Southard RJ, Claassen VP. 2009. Plant-available calcium varies widely in soils on serpentinite landscapes. Soil Sci Soc Am J 73:2087-95.

McGrath SP. 1995. Chromium and nickel. In Alloway BJ, editor. Heavy metals in Soils, 2nd ed. London: Blackie Academic and Professional. p 152-78.

McLean EO. 1982. Soil pH and lime requirement. In: Page AL, Miller RH, Keeney DR, editors. Methods of soil analysis, Part 2. 2nd ed. Agronomy Monographs 9. Madison, WI: Agronomy Society of America and Soil Science Society of America. p 199-224.

Mehra OP, Jackson ML. 1960. Iron oxides removed from soils and clays by a dithionite-citrate system buffered with sodium bicarbonate. Clay Clay Miner 7:317-27.

Mills CT, Morrison JM, Goldhaber MB, Ellefsen KJ. 2011. Chromium(VI) generation in vadose zone soils and alluvial sediments of the southewatern Sacramento Valley, California: a potential source of geogenic Cr (VI) to groundwater. Appl Geochem 26:1488-501.

Miranda M, Benedito J, Blanco-Penedo I, López-Lamas C. 2009. Metal accumulation in cattle raised in a serpentine-soil area: relationship between metal concentrations in soil, forage and animal tissues. J Trace Elem Med Biol 23:231-8.

Nelson DW, Sommer LE. 1982. Total carbon, organic carbon, and organic matter. In: Page AL, Miller RH, Keeney DR, editors. Methods of soil analysis, Part 2. 2nd ed. Agronomy Monographs 9. Madison, WI: Agronomy Society of America and Soil Science Society of America. p 539-77.

O'Hanley DS. 1996. Serpentinites: records of tectonic and petrological history. New York: Oxford Univ. Press. 277 p.

Oze C, Fendorf S, Bird DK, Coleman RG. 2004. Chromium geochemistry of serpentine soils. Int Geol Rev 46:97-126.

Proctor J, Woodell SRJ. 1971. The plant ecology of serpentine: I. Serpentine vegetation of England and Scotland. J Ecol 59:375-95.

Rabenhorst MC, Foss JE. 1981. Soil and geologic mapping over mafic and ultramafic parent materials in Maryland. Soil Sci Soc Am J 45:1156-60.

Rabenhorst MC, Foss JE, Fanning DS. 1982. Genesis of Maryland soils formed from serpentinite. Soil Sci Soc Am J 46:607-16.

Rhoades JD. 1982. Cation exchange capacity. In: Page AL, Miller RH, Keeney DR editors. Methods of soil analysis, Part 2. 2nd ed. Agronomy Monographs 9. Madison, WI: Agronomy Society of America and Soil Science Society of America. p 149-57.

Robertson AI. 1985. The poisoning of roots of *Zea mays* by nickel ions, and the protection afforded by magnesium and calcium. New Phytol 100:173-89.

Soil Survey Staff. 1993. Soil survey manual. US Department of Agriculture. Handbook. no. 18. Washington, DC: US Government Printimg Office. 437 p.

Soil Survey Staff. 2010. Keys to Soil Taxonomy, 12th ed. Washington, DC: Natural Resources Conversation Services, US Department of Agriculture. 332 p.

Wu Y, Hendershot WH. 2010. The effect of calcium and pH on nickel accumulation in and rhizotoxicity to pea (*Pisum sativum* L.) root–empirical relationships and modelling. Environ Pollut 158:1850-6.